THE JOURNAL OF PHYSICAL CHEMISTRY B

Article

pubs.acs.org/JPCB

Solution Phase Exciton Diffusion Dynamics of a Charge-Transfer Copolymer PTB7 and a Homopolymer P3HT

Sung Cho,[†,‡,§] Brian S. Rolczynski,[†,‡] Tao Xu,[∥] Luping Yu,*[,∥] and Lin X. Chen*[,†,‡]

[†]Chemical Sciences and Engineering Division, Argonne National Laboratory, Argonne, Illinois 60439, United States

[‡]ANSER Center and Department of Chemistry, Northwestern University, 2145 Sheridan Road, Evanston, Illinois 60208, United States

[§]Department of Chemistry, Chonnam National University, Gwangju 500-757, Korea

[∥]Department of Chemistry and the James Franck Institute, The University of Chicago, 929 East 57th Street, Chicago, Illinois 60637, United States

Supporting Information

ABSTRACT: Using ultrafast polarization-controlled transient absorption (TA) measurements, dynamics of the initial exciton states were investigated on the time scale of tens of femtoseconds to about 80 ps in two different types of conjugated polymers extensively used in active layers of organic photovoltaic devices. These polymers are poly(3-fluorothienothiophenebenzodithiophene) (**PTB7**) and poly-3-hexylthiophene (**P3HT**), which are charge-transfer polymers and homopolymers, respectively. In **PTB7**, the initial excitons with excess vibrational energy display two observable ultrafast time constants, corresponding to coherent exciton diffusion before the vibrational relaxation, and followed by incoherent exciton diffusion processes to a neighboring local state after the vibrational relaxation. In contrast, **P3HT** shows only one exciton diffusion or conformational motion time constant of 34 ps, even though its exciton decay kinetics are multiexponential. Based on the experimental results, an exciton dynamics mechanism is conceived taking into account the excitation energy and structural dependence in coherent and incoherent exciton diffusion processes, as well as other possible deactivation processes including the formation of the pseudo-charge-transfer and charge separate states, as well as interchain exciton hopping or coherent diffusion.

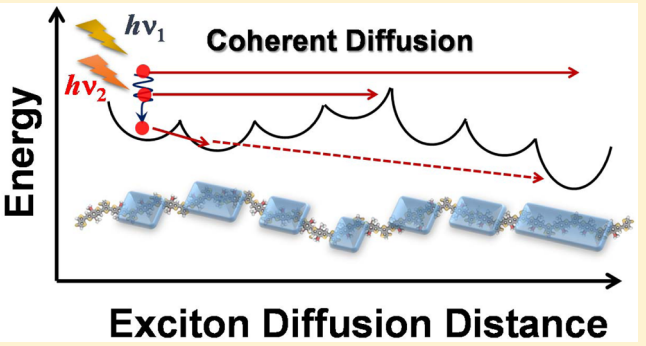

I. INTRODUCTION

Since the first solar cell with an all-organic active layer was created more than three decades ago, conducting polymers have emerged as one of the most important materials in molecular photonics, such as solar cells, optoelectronic switches, and organic light-emitting diodes.[1−5] In particular, considerable efforts have been devoted to organic photovoltaics (OPV) to generate solar electricity for future energy demands.[4,6] Bulk heterojunction (BHJ) OPV devices have various advantages: low cost, easy fabrication, and minimal environmental impact compared to silicon, precious metal, or inorganic solar cells based on toxic elements.[7,8] In the past five years, the power conversion efficiency (PCE) of OPV devices has doubled to over 10%, which is a great leap forward toward large-scale device commercialization.[9] Extensive use of conjugated charge transfer copolymers plays an important role in the recent PCE improvements.

OPV function is conventionally described by the following steps: (1) light harvesting by a conjugated polymer in the active layer to generate excitons, (2) exciton diffusion to an interface/junction of the electron donor/acceptor (e.g., polymer/fullerene), (3) charge separation at the interface/junction, (4) charge-carrier diffusion through the active layer, and (5) charge collection by corresponding electrodes.[10−12] Because these steps take place sequentially, losses at each step can be responsible for a low device PCE. In order to construct a high-efficiency OPV device, optimization at the aforementioned strongly correlated, sequential steps is needed. Recent advances in understanding the BHJ OPV device mechanisms have raised several important questions, leading to re-evaluation of the OPV conventional wisdom. For example, the nature of the initial exciton dynamics and subsequent exciton diffusion/delocalization in OPV polymers are still not well-understood due to the polymer structural complexity and inhomogeneity in the BHJ films, which obscure the optical features for the intermediate species of interest. The intrinsic local conformational variations of a polymer backbone also induce

Special Issue: John R. Miller and Marshall D. Newton Festschrift

Received: November 6, 2014
Revised: January 24, 2015

DOI: 10.1021/jp5111345
J. Phys. Chem. B XXXX, XXX, XXX−XXX

inhomogeneous broadening in exciton energies. Consequently, the transient spectral features for other intermediates that evolved from these exciton populations are also broad and overlap with each other, which makes OPV dynamics measurements ambiguous. Moreover, exciton delocalization or diffusion occurs simultaneously with energy relaxation, and the two processes can be strongly intertwined and hard to distinguish from ultrafast optical transient absorption (TA) signals alone. In this report, we investigated exciton energy relaxation and diffusion dynamics of two conjugated polymers with different local structures to reveal the nature of the initial and relaxed exciton states within 100 fs after photoexcitation. Although time-resolved fluorescence techniques have been used to investigate exciton energy relaxation dynamics, the initial exciton state and its ultrafast dynamics within 100 fs could not be measured accurately because the detected emission energies mainly originate from partially or fully relaxed emissive excitons rather than from the initial exciton states.[13,14] To circumvent this limitation, we used single-color pump−probe transient absorption (TA) and transient absorption anisotropy (TAA) techniques to monitor the generation of the initial exciton state and subsequent deactivation processes with precisely controlled conditions of initial excited states under various excitation energies. Using this method, the initial and relaxed exciton dynamics in two representative OPV polymers were investigated. Poly(thienothiophenebenzodithiophene) (**PTB7**) is a charge transfer polymer in which each repeating unit contains two building blocks with electron-donating (benzodithiophene, **BDT**) and electron-withdrawing (thienothiophene, **TT**) character; and poly-3-hexylthiophene (**P3HT**) is a typical conjugated homopolymer with identical building blocks along the entire polymer backbone (Scheme 1). Exciton diffusion

Scheme 1. Molecular Structures of PTB7 and P3HT

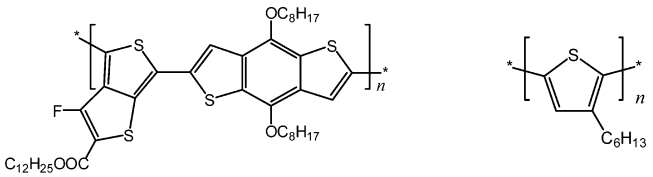

PTB7 P3HT

dynamics have been extensively studied; however, connections of the exciton diffusion/delocalization dynamics with the local structure, chemical composition, and conformation along the polymer backbone are still not completely clear. Recent findings on exciton dissociation within <100 fs in the active layer of bulk heterojunction (BHJ) devices[15,16] and in PTB7 solutions[17] suggest the importance of studying exciton dynamics in terms of exciton delocalization and diffusion before vibrational relaxation. **PTB7** and **P3HT** are chosen in this study because they represent two types of conjugated polymers differing in both electronic and conformational structures. **PTB7** is a charge-transfer conjugated polymer, defined as a polymer whose repeating motif has distinct aromatic building blocks: **BDT** and **TT** with electron-donating and -withdrawing characters, respectively. This polymer is rather rigid in solution and has tendency to aggregate, as suggested by a close resemblance in the absorption spectra with those of its solid films. It has been shown that the exciton in charge transfer polymers have intrinsic local polarity due to the electron push−pull actions by donor and acceptor blocks in each repeating unit, which enables the ultrafast exciton dissociation in solution[17] and in BHJ films.[18] In contrast, **P3HT** is a homopolymer with no significant charge transfer character along the backbone, and it is rather conformationally disordered and flexible in solution, as demonstrated by the broad absorption features and their drastic transformation in solid films to significantly red-shifted absorption peaks with clearly visible vibronic features.

In this report, we investigate the nature and dynamics of the excitons with different polymer conformational distribution, local electronic structure, and initial exciton energetics. We hope to decipher the exciton dynamics in these two polymers and use the finding to understand how the intrinsic charge transfer characters along the polymer chain influences the exciton dynamics and how such influence will affect the OPV device efficiency.

II. EXPERIMENTAL METHODS

Materials and Synthesis. **PTB7** polymer was synthesized according to the procedure in previous literature.[19] **P3HT** was purchased from Sigma-Aldrich. The reference compound for experimental setup calibration, **Oxazine 725**, was obtained from Exciton. The solvents for the polymers, toluene and chlorobenezene, were purchased from Sigma-Aldrich. All purchased materials were used without further purification.

Steady-State Electronic Absorption Spectrum Measurements. Steady-state UV−vis absorption spectra were measured by a Shimadzu spectrophotometer (UV-3600). **PTB7** and **P3HT** in toluene or chlorobenezene solutions were used at room temperature and purged with nitrogen.

Time-Resolved Transient Absorption Measurement. A femtosecond time-resolved single-color transient absorption (TA) apparatus consisted of a visible collinear optical parametric amplifier (OPA) pumped by a Ti:sapphire regenerative amplifier laser (RegA9000, Coherent Lasers) and an optical detection system.[20] The output beam from the RegA had a power of about 1.5 W at a repetition rate of 150 kHz, which was used to pump an optical parametric oscillator (OPA, Coherent) to create ultrafast pulses in the region of 490−700 nm. The resulting laser pulses had a temporal width of ∼50 fs fwhm measured through autocorrelation at the sample position by optical Kerr effect signal of MeOH.[20] The spectral width of the pulse was about 400 cm^{-1}. The pump and probe beams were focused and overlapped at the sample solution in a 2 mm path cuvette. The time delay between the pump and the probe pulses was controlled by a variable optical delay line. In order to prevent photodegradation of polymers and to minimize multiphoton processes, such as exciton−exciton annihilation, the pump pulse intensity has been attenuated for all wavelengths by using variable neutral density filter, and so was the probe intensity with about 1/8 of the pump energy. The pump and probe intensities of 0.64 mW (4.3 nJ/pulse) and 0.08 mW (0.53 nJ/pulse) were respectively used in the measurements with optimized experimental condition for single-color TA experiment. The polarization directions of the pump and probe beams were selected by varying the orientations of half-wave plates ($\lambda/2$) and linear polarizers. The polarization of the pump beam was vertical, whereas the polarization of the probe beam was at 45° relative to the vertical. After the sample, the polarized signals of the parallel ($I_{\parallel}$) and perpendicular ($I_{\perp}$) to the polarization of the pump beam were separated by a cube polarizer and then recorded simultaneously by using two silicon photodiodes and two lock-

DOI: 10.1021/jp5111345
J. Phys. Chem. B XXXX, XXX, XXX−XXX

in amplifiers. Finally, the magic angle (I_M) and anisotropy (r) traces were obtained using the following equations:

$$I_M = \frac{I_{II} + 2I_{\perp}}{3}, \quad r = \frac{I_{II} - I_{\perp}}{I_{II} + 2I_{\perp}} \tag{1}$$

As a precaution against unwanted interference near time zero between the pump and probe, a dye molecule reference, **oxazine 725** was used to ensure that the sample geometry is free of such interference and that the initial anisotropy of the dye is about 0.36.

Theoretical Calculations. The molecular structures of oligomers mimicking the corresponding polymers were optimized by low- (Hartree−Fock (HF) Hamiltonian with 3-21G basis set) to high level (Density Function Theory (DFT) B3LYP Hamiltonian with 6-31G* basis set) in a stepwise manner, and then the electronic states of **PTB7** and **P3HT** oligomers were calculated using time-dependent DFT (TDDFT) with the B3LYP Hamiltonian and 6-31G* basis to obtain the electronic transition energies and oscillator strengths of the excited states. The initial structures of the **PTB7** and **P3HT** oligomer analogs were optimized from the optimized constituent blocks; **TT** and **BDT** for **PTB7** oligomer and a thiophene for **P3HT** oligomer, and then the number of blocks was increased step by step. To simplify the calculations and reduce the computation time, the alkyl side groups on building blocks in **PTB7** and **P3HT** were truncated to methyl groups. Excited state calculations were performed on the optimized ground state structures using time-dependent density functional theory at the B3LYP/6-31G* level of theory.

III. RESULTS

Steady-State Absorption Spectra. Figure 1 shows the steady-state absorption spectra of **PTB7** and **P3HT** in toluene.

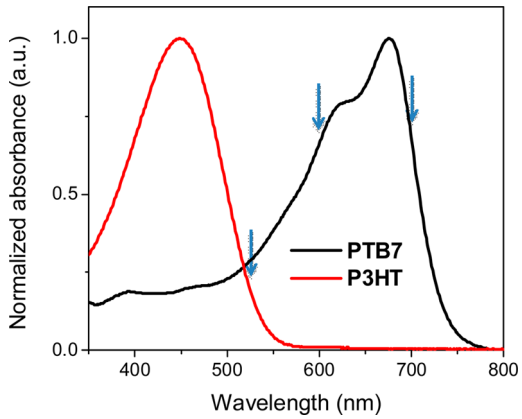

Figure 1. Steady-state absorption spectra of **PTB7** and **P3HT** in toluene. The excitation wavelengths of 600 and 700 nm, respectively, for **PTB7** and 510 nm for **P3HT** used for the TA measurements are marked by blue arrows.

While **P3HT** shows a broad and featureless absorption band peaked around 450 nm, **PTB7** exhibits two distinct peaks at the center wavelengths of 625 and 685 nm, respectively. The energy difference between two peaks is ~0.182 eV (Table 1), which corresponds to the vibrational energy of the C=C stretching mode of 0.186 eV or 1500 cm^{-1},[21,22] and hence, the two peaks are assigned to the 0−0 and 0−1 vibronic bands for the $S_1 \leftarrow S_0$ transition. The broad and featureless absorption spectrum (fwhm ~2660 cm^{-1}) of **P3HT** has been attributed to diverse local conformations due to the variations in dihedral angles between two adjacent thiophene units along the conjugated backbone,[23,24] which causes variations in interunit π-conjugation strength and length, resulting in excited states with broadly distributed energy levels.[5] In comparison, the absorption spectrum of **PTB7** has a narrower absorption band (fwhm ~1105 cm^{-1}) with distinct vibronic peaks, suggesting its more homogeneous local structures even in solution, likely sustained by both quinoical characters in the conjugated backbone as well as interbackbone aggregation. In this report, we used two excitation wavelengths of 600 and 700 nm for **PTB7**, preferentially exciting the 0−1 and 0−0 vibronic bands in the $S_1 \leftarrow S_0$ transition, respectively, and one excitation wavelength of 510 nm for **P3HT**, exciting preferentially the 0−0 vibronic band, to investigate effects of excess vibrational energies in exciton relaxation and diffusion dynamics. When a conjugated polymer is excited by photons at higher energies than the onset of the absorption band, inhomogeneous distributed initial exciton states are created that can be represented by the two extreme situations: (1) the lower energy initial exciton states located at a longer conjugated segments of the polymer with more excess energy and (2) the higher energy initial exciton states at shorter conjugated segments of the polymer with less excess energy. Therefore, the dynamics of the initial exciton states of **P3HT** are intrinsically inhomogeneous if the excitons are created by photons with higher energy (e.g., 400−450 nm) than the red-edge of the absorption band. In order to reduce the inhomogeneity of the initial excitons of **P3HT**, we chose photoexcitation at 510 nm, near the red edge of the absorption spectrum, to preferentially generate the initial excitons of long conjugated segments with minimal excess energy. Based on a similar assumption, we used the photoexcitation at 700 nm near the red edge of the **PTB7** absorption to generate more homogeneous initial excitons in **PTB7**. Because **PTB7** has more rigid and, hence, more homogeneous, local structures than **P3HT** in solution, it is a preferred system to investigate the effect of excess energy alone on the exciton dynamics, separating the effects of structural reorganization when the initial exciton state is created using shorter excitation wavelength at 600 nm.

Optimized Molecular Structures of PTB7 and P3HT Oligomers. **PTB7** and **P3HT** differ by their repeating unit sequences, alternating (-A-B-A-B-) versus homo (-A-A-A-A-). Figure 2A,B shows the optimized molecular structures of **PTB7** and **P3HT** oligomers. Although two 2,5-linked adjacent thiophenes are at an angle, the overall shape of regioregular **P3HT** oligomer is close to linear. In contrast, the overall shape of the **PTB7** oligomer backbone is zigzag. According to the calculated structures in vacuo, the oligomer thiophene are perfectly coplanar while the oligomer **BDT-TT** are not in the same plane but have an average dihedral angle of 21.4° between the two adjacent repeating units. The steric hindrance between **TT** and **BDT** in **PTB7** presumably restricts the rotational motion and reduce the variation of dihedral angles between them. Also, **TT** induces the quinoidal character or bond order increase on the C−C bond connecting building blocks, which also enhances the rigidity along the **PTB7** backbone. Thus, **PTB7** in solution exhibits a narrow absorption spectrum with distinct vibronic features. Conversely, **P3HT** cannot maintain a coplanar structure in solution because the low energy barriers for the relative rotations along the connection C−C bond between two thiophenes, resulting in a variety of local

DOI: 10.1021/jp5111345
J. Phys. Chem. B XXXX, XXX, XXX−XXX

Table 1. Fitting Parameters of PTB7 and P3HT Exciton Dynamics in Toluene

			TA				
compd	solvent	absorption peak position (nm; width/cm^{-1})	excitation and probe wavelength (nm)	τ_1 (amp.)	τ_2 (amp.)	τ_3 (amp.)	τ_4 (amp.)
PTB7	toluene	680.3 (1105), 618.6 (1525)	600	34 ± 5 fs (50.1%)	1.85 ± 0.13 ps (4.0%)		504 ± 11 ps (45.9%)
			700	100 ± 5 fs (43.0%)	1.90 ± 0.08 ps (4.9%)	42.1 ± 3.2 ps (6.6%)	505 ± 22 ps (45.5%)
P3HT	toluene	468.6 (2660)	510	55 ± 10 fs (70.0%)	1.33 ± 0.16 ps (12.1%)	15.2 ± 1.2 ps (15.2%)	long (2.7%)

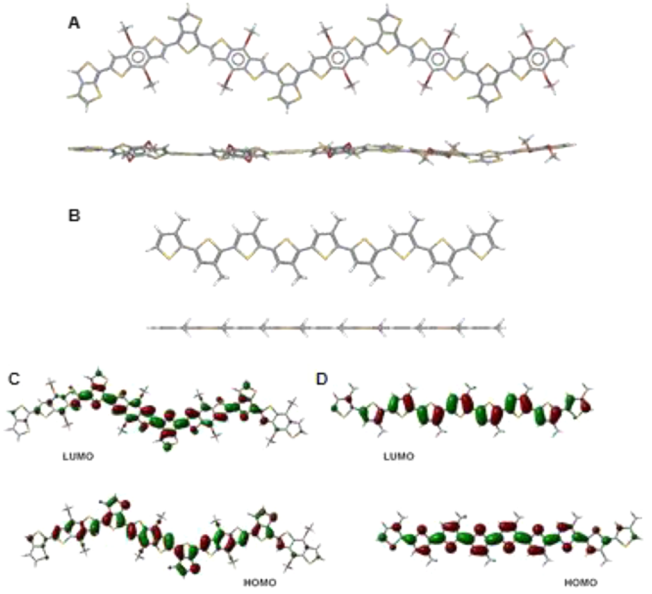

Figure 2. Optimized molecular structures (A, B) and the HOMOs and LUMOs (C, D) of **PTB7** and **P3HT** oligomers, respectively.

conformations and hence a broad absorption peak for the lowest energy transitions. The calculated energy barrier for a rotation of the C−C bond connecting the two adjacent thiophene units from 0° (planar) to 90° (orthogonal) is ∼1.5 kcal/mol, as reported by Friesner and co-workers on dithiophenes with methyl or ethyl at 3,4′ positions.[25] Consequently, **P3HT** chain in vacuo has low potential barriers for the rotation along the C−C bonds between two adjacent units, enabling the coexisting variety of conjugation lengths. Such conformational flexibility apparently has translated to the solution case. In comparison, the rotation along the C−C bond connecting **BDT** and **TT** blocks in a single repeating unit of **PTB7** is ∼3 kcal/mol,[26] which will be more likely to stiffen the polymer backbone. Hence, the overall structure of **PTB7** in solution is more homogeneous compared to **P3HT**. However, the above comparison is mostly qualitative since the local conformation is often defined by more than just one rotation along the C−C bond and the steric hindrance of the side chain truncated in the computation could also influence the energy barriers for the C−C bond rotation.

As shown in Figure 2C,D, the highest occupied molecular orbitals (HOMOs) and lowest unoccupied molecular orbitals (LUMOs) for **PTB7** and **P3HT** oligomers differ significantly in terms of electron density delocalization. The respective sets of HOMOs and LUMOs for the two oligomers represent the main differences between an alternating copolymer and a homopolymer. While the **P3HT** oligomer exhibits the delocalized HOMO and LUMO over the entire oligomer except the two terminal thiophene units, the location of HOMO and LUMO are the same. In comparison, the frontier HOMO and LUMOs of **PTB7** oligomer are less delocalized and displaced from one and another along the conjugated backbone, suggesting the displacement of electron deficient and electron region, resulting in intrinsic polarity in their excitons.[17,27,28] Therefore, the overall inter-repeating unit interactions in the **PTB7** oligomer are more localized than those in the **P3HT** oligomer. Because the adjacent **TT** and **BDT** blocks in **PTB7** oligomer are energetically different, the electronic coupling between them will be weaker than that between two identical blocks, resulting in electronic potential gradients and hence energy barriers for the $2p_z$ electrons to delocalize. From TDDFT calculations, the transition energy of the S_1 state of a **TT-BDT** pentamer analogous to **PTB7** is 1.886 eV (657.6 nm) with the apparent delocalization of the wave functions over 3−4 repeating units, which is close to the real peak position of the $S_1 \leftarrow S_0$ transition energy in the absorption spectrum of **PTB7** in solution, suggesting that the electron delocalization through the backbone is about 3−4 repeat unit long on the basis of the saturated HOMO−LUMO gap and TDDFT calculation. Therefore, the energy gap reduction as a function of the oligomer length is less drastic in the charge-transfer copolymer **PTB7** compared to the same trend in the oligomer depicting **P3HT** because of much weaker interactions across the repeating units along the **PTB7** backbone.

The calculated $S_1 \leftarrow S_0$ transition energy for **PTB7** oligomer is 1.886 eV (657.6 nm, with an oscillator strength $f = 4.2941$) and for **P3HT** oligomer, 2.072 eV (598.5 nm, and $f = 3.0473$). Both are optically allowed, whereas their corresponding S_2, $S_3 \leftarrow S_0$ transitions for **PTB7** oligomer are at 2.130 eV (582.1 nm, $f = 0.0080$) and 2.182 eV (568.3 nm, $f = 0.0109$), and for **P3HT** oligomer, 2.448 eV (506.6 nm, $f = 0.0000$) and 2.647 eV (468.4 nm, $f = 0.0003$) are optically forbidden. These results also support the assignments of the two lowest energy absorption features of **PTB7** as the vibronic bands of the S_1 state. In addition, a large energy discrepancy between the calculated $S_1 \leftarrow S_0$ states transition energy (2.072 eV) for a planar **P3HT** nonamer and the observed absorption band of **P3HT** in solution (2.638 eV) suggests that **P3HT** in solution adopts conformations far from planar, in agreement with the literature.[14]

Isotropic Transient Absorption (TA) Profiles. Figure 3 shows single-color TA signals for **P3HT** and **PTB7** in toluene, at room temperature and under different excitation energies. Because the signs of TA signals of **PTB7** and **P3HT** are both negative, the origins of the TA signals can be the ground-state bleaching (GSB) and stimulated emission (SE).

Excitation at the Red-Edge of the Absorption Spectra. The red edges of the TA signals for **PTB7** and **P3HT**, at 700 and 510 nm, respectively, were each fit to a linear combination of

DOI: 10.1021/jp5111345
J. Phys. Chem. B XXXX, XXX, XXX−XXX

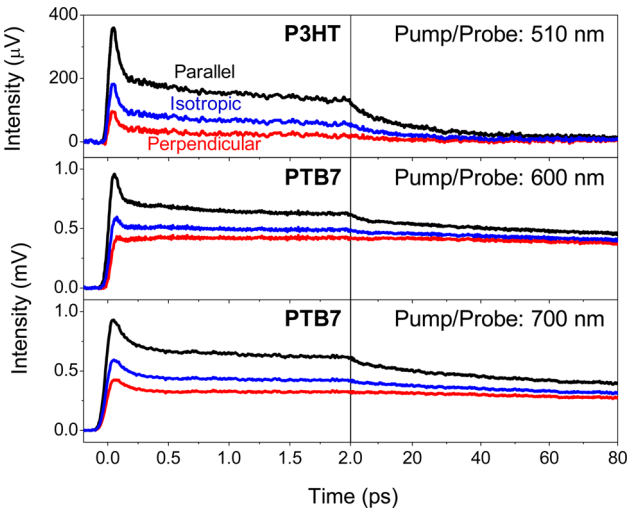

Figure 3. Parallel, perpendicular, and isotropic TA signals for PTB7 in toluene at room temperature after photoexcitation at 700 nm.

exponential functions, yielding parameters summarized in Table 1. The TA signal of **P3HT** fits a sum of four exponential functions with corresponding time constants of 55 fs, 1.33 ps, 15.2 ps, and a fourth component with a time constant longer than the experimental time window. These time constants are in good agreement with the previously reported experimental results for exciton dynamics of **P3HT** in solution.[13,14] The origin of the long component is likely from SE of the fully relaxed S_1 exciton state, and GSB. Because **P3HT** in solution exhibits long singlet and triplet lifetimes of 600 ps and 300 ns, respectively,[21] we deduce that the three fast decay components of **P3HT** are from SE of the initial and partially relaxed excitons because the GSB recovery of **P3HT** takes at least 600 ps.

The isotropic TA signal of **PTB7** also shows four exponential decay components of 100 fs, 1.9 ps, 42 ps, and ~500 ps. The longest component was extrapolated based on the high quality experimental data and its substantial amplitude still remained at the end of the 80 ps time window. Interestingly, the time scales of these time constants from the fits for **PTB7** and **P3HT** are similar under the red-edge excitation, suggesting a similarity in their exciton relaxation dynamics in spite of differences in molecular structures. Therefore, it is reasonable to assume that the longest component of ~500 ps in **PTB7** originates from the fully relaxed S_1 state, and the three fast components are also from SE from the initial and partially relaxed excitons. Although we did not measure the triplet state lifetime, this value has been shown in the literature to be about 300 ns in aerated solution,[29] which is much shorter than the temporal separation of 6.67 μs between the two consecutive pump pulses. The populations of the initial excitons are generated instantaneously in **PTB7** and **P3HT**; and the negative signs of the three fast decay components are mostly caused by the SE process from the initial and partially relaxed excitons, because the SE is an emissive process and only takes place by bound electron−hole pairs. Consequently, we conclude that our isotropic TA data of **PTB7** and **P3HT** reveal the dynamics of excitons, and that the initial excited state can be monitored by our experimental tool, because the selection rules of absorption and emission processes are the same and subsequently the initial state after photoexcitation is emissive.

Photoexcitation with Excess Energy. Compared with the exciton dynamics under the red-edge excitation at 700 nm, the fastest exciton decay component of **PTB7** becomes even faster under the higher energy excitation at 600 nm corresponding to approximately one vibrational quanta excess in energy, while the other time constants are nearly the same (Table 2). The faster decay time of 34 fs in the shortest time constant suggests that there are additional deactivation pathways when there is an excess in the excitation energy. Recently, Rolczynski et al. reported that a portion of the exciton forms the pseudocharge-transfer (PCT) and charge-separated (CS) states within 160 fs after the excitation in presumably isolated **PTB7** in solution.[17] Since nominal exciton binding energies can be as low as ≤0.1 eV in some charge transfer copolymers,[5] it is conceivable that a considerable excess energies in the exciton could enable the ultrafast exciton dissociation if the process competes favorably with the vibrational relaxation. Consequently, some initial excitons can dissociate via intra- or interchain processes and then transform to PCT and CS states in solution before thermal/vibrational relaxation, even without the electron acceptor, **PCBM** (phenyl-$C_{61/71}$-butyric acid methyl ester). In comparison, such exciton dissociation processes are rare in homopolymers in solution due to their much higher exciton binding energies. If the fastest isotropic TA decay component of the charge transfer **PTB7** under the 700 nm excitation

Table 2. Fitted TAA Parameters of PTB7, P3HT, and Oxazine 725

			anisotropy[a] (TAA)					
							amplitude	
compd	solvent	excitation and probe wavelength/nm	τ_1 (amp.)	τ_2 (amp.)	τ_3 (amp.)	τ_4 (amp.)	r_∞	r_{total}
PTB7	toluene	600	41 ± 5 fs (0.126)	324 ± 10 fs (0.053)	2.68 ± 0.05 ps (0.044)	26.9 ± 0.4 ps (0.042)	0.092	0.357
		700	35 ± 5 fs (0.063)		2.57 ± 0.04 ps (0.059)	30.0 ± 0.5 ps (0.085)	0.124	0.331
	CB	600	39 ± 10 fs (0.124)	319 ± 10 fs (0.052)	2.78 ± 0.05 ps (0.042)	30.7 ± 0.6 ps (0.038)	0.097	0.353
		700	26 ± 5 fs (0.098)		2.44 ± 0.05 ps (0.052)	28.1 ± 0.5 ps (0.077)	0.124	0.351
P3HT	toluene	510				34.3 ± 1.1 ps (0.306)	0.022	0.328
Oxazine 725	MeOH	600				63.9 ± 6.0 ps (0.361)		0.361

[a]The TAA signals fit exponential functions from 80 fs to 80 ps to avoid the effect of the pump-induced signal and the instrumental response function (IRF) is shown in parentheses after the time constant.

DOI: 10.1021/jp5111345
J. Phys. Chem. B XXXX, XXX, XXX−XXX

corresponds mainly to the intravibrational band relaxation, the even faster decay of the TA signal under the 600 nm excitation is probably due to the exciton dissociation to PCT and CS states through intrachain processes, which will be in favor when there is an excess of energy. The exciton dissociation process from the initial excitons can take place as fast as 50 fs, which has also been observed by other groups.[16] Therefore, we suggest that the initial states of **PTB7** and **P3HT** are emissive and that the exciton dissociation of the initial excitons in **PTB7** may be enhanced when the initial excitons have enough excess vibronic energy before the vibrational relaxation. Because the fastest time constants are only 100 fs or less, such an effect can only be detected when the pump−probe pulses are sufficiently short. Our previous studies with a 160 fs (fwhm) instrumental response function (IRF) could not detect the excitation wavelength dependent exciton dynamics in isolated **PTB7** in solution.[17]

Transient Absorption Anisotropy Profiles. Although isotropic TA results provide initial exciton dynamic information, their connections to exciton diffusion process are still unclear. Transient absorption anisotropy (TAA) signals measure the autocorrelation function of the transition dipole moment vector, which is sensitive to dynamic processes causing the anisotropy to diminish, such as exciton diffusion along a randomly oriented polymer backbone or across different chains in π-stacked aggregates and deactivation of the excitons by electron transfer or chemical reactions. The relevant depolarization processes considered can be related to the exciton diffusion along a winding polymer chain or between π-stacked chains, as shown by Rossky and co-workers,[30,31] which will disrupt the original dipole moment orientation along the backbone, as well as polymer motions in solution which randomize the dipole moment orientation. If an exciton stays in one location in the experimental window, the initial anisotropy at time zero $r(0)$ should be close to 0.4 and the decay constant for $r(t)$ would be rather long mainly due to the molecular motions of the polymer chain that could scramble the dipole orientation. If the exciton diffuses along a rigid polymer chain, $r(t)$ will have a longer decay time constant then if the exciton diffusion takes place in a randomly coiled or flexible polymers. Therefore, one can use the $r(t)$ dynamics to correlate with the exciton diffusion process along the polymer chains. Interestingly, TAA signals of **PTB7** and **P3HT** have distinctly different dynamic behaviors even their normal TA signals corresponding to the exciton decay dynamics have similar time constants (Figure 4). Within the same experimental time window of 80 ps, the $r(t = 80\ \text{ps})$ values for **PTB7** is about five times larger than that of **P3HT**, even though **PTB7** has shown substantial depolarization processes within a few picoseconds which is likely related to exciton diffusion (Table 2). The fast exciton diffusion and long lasting TAA signal seem to be contradictory because the exciton diffusions in flexible polymer chains in solution can randomize the exciton dipole orientation. The above contradiction can only be explained if **PTB7** is more rigid and linear than **P3HT** in solution, which also agrees with our calculated results on the optimized oligomer structures of **PTB7** and **P3HT**. Huo at al. reported that the excitons and the CS states inhabit the stretched strands and the thermally robust orderly stacked domains in PBDTTT copolymers.[29] The relatively rigid and stretched local structure of **PTB7** can be an important reason for efficient exciton diffusions through the polymer backbone while π-stacked interchain aggregation could open another route for exciton diffusion. Also observed was the

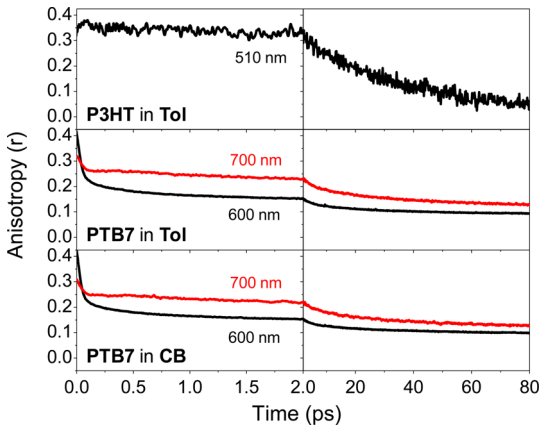

Figure 4. TAA signals for P3HT in toluene and PTB7 in toluene and CB at room temperature after photoexcitation at 510, 600, and 700 nm, respectively.

excitation energy-dependent TAA dynamics of **PTB7**. Under the 600 nm light excitation, which has a photon energy higher than that at 750 nm, the absorption onset, the amplitude of the first fast decay component in the TAA signal becomes larger and a new decay component appears with a time constant of 324 fs. Since the probe wavelength at 600 nm corresponds to the $S_1(v = 1) \leftarrow S_0(v = 0)$ vibronic transition, the transition dipole moments of two vibronic bands at 619 and 680 nm are the same. Hence, the excitation wavelength dependent **PTB7** TAA signals under the 600 and 700 nm excitations are presumably related to the exciton behaviors with and without an excess of one vibrational quanta, respectively.

IV. DISCUSSION

Our experimental results have demonstrated that the initial excitons generated via optically allowed transitions undergo multiple relaxation pathways to different electronic states, the PCT and CS states, and vibrational relaxed/thermally equilibrated exciton states. During the energetic relaxation processes, the excitons in **PTB7** can migrate to different isoenergetic or lower energy sites. Since the energetic relaxation of the excitons and the transition dipole moment reorientation due to the exciton migration are concurrent phenomena, it is challenging via TA measurements alone to distinguish between the mobile exciton migration and the stationary exciton energetic deactivation within a polymer backbone if these phenomena occur on similar time scales. Considering the exciton diffusion along a flexible polymer chain in solution, the exciton mobility can be extracted from reorienting dynamics of transition dipole moments and the absorption/emission anisotropy values. By selecting the photoexcitation energies, we can preferentially create excitons of different initial vibronic states to extract dynamics information on the energetic deactivation and exciton diffusion in the S_1 states of **PTB7** and **P3HT** based on their respective SE signals from the S_1 state. Meanwhile, if the π-stacked aggregation due to single chain folding takes place, the anisotropy decay can originate from the depolarization of the transition dipole moment from near perpendicular directions of the dipole moment along the backbone and exciton hopping through the interchain π-stack. However, according to the results of exciton diffusion in single P3HT chain by Hu et al.,[30] such a process is only significant in a relatively long-range ordered π-stack but is attenuated in the aggregate with only a few π-stacked chains. Based on our

DOI: 10.1021/jp5111345
J. Phys. Chem. B XXXX, XXX, XXX−XXX

previous grazing incident angle and solution X-ray scattering studies, the aggregation in **PTB7** can be locally ordered with 6−7 π-stacked chains in solid film while the majority of the polymers, despite forming aggregates, are largely disordered in both solid films and solution.[27,32] Therefore, the π-stack in solution for **PTB7** can be even more disordered and the interchain exciton diffusion will not be a major route. With the above considerations in mind, the depolarization components in the TAA traces of **PTB7** and **P3HT** as a function of the photoexcitation energy can be directly connected to the exciton diffusion and structural deformation, whereas the isotropic TA signals are mostly resulted from the energetic relaxation of localized or mobile excitons.

To analyze experimental results, we made two assumptions. First, all exciton relaxation dynamics start from the S_1 state, the lowest energy exciton state, because the chosen pump wavelength of 510 nm for **P3HT** and those of 600 and 700 nm for **PTB7** induce the $S_1 \leftarrow S_0$, transitions in the two polymers, respectively. Second, there are at least three possible transient states, exciton, PCT, and CS states as shown in our previous studies.[17,28] As mentioned earlier, the three fast decay components in TA traces of **PTB7** and **P3HT** are mainly from SE signals, emissive excitons are probed by our single-color TA measurements. Therefore, the isotropic TA and TAA traces reflect the energetic relaxation and depolarization processes of excitons, respectively. If the PCT state can be approximated as a weakly bounded exciton state and the CS state is nonemissive, the contributions of the PCT and CS states to SE signal are presumably negligible.

For **PTB7**, the time scales of the energetic relaxation and depolarization components in isotropic TA and TAA traces, respectively, are similar, indicating that the energetic relaxation and exciton diffusion processes are strongly correlated. In contrast, **P3HT** shows totally different dynamics in the isotropic TA and TAA traces, suggesting that the fast energetic relaxation processes seen in the former are not involved in the exciton diffusion and are mainly due to the energetic relaxation of stationary excitons.

Exciton Dynamics in P3HT. The single exponential in the TAA decay kinetics of **P3HT** reveals that there is only one major depolarization process even though there can be multiple exciton relaxation processes shown in the isotropic TA decay kinetics. This observation shows that the two fast energetic relaxation processes extracted from the isotropic TA signal are not related to the dipole moment reorientation due to the exciton diffusion, structural deformation or any other processes causing the depolarization of the TAA signals. However, multiple depolarization processes and fast exciton diffusion within 1 ps in **P3HT** were reported by previous works using fluorescence measurements.[14,33,34] The discrepancy can be explained by different initial exciton states created under different experimental conditions. Because the coplanar conformation in a conjugated polymer optimizes the overlap of parallel $2p_z$ orbitals of carbon atoms along the polymer chain, and the energy gap between HOMO and LUMO decreases with the number of carbon atoms in a conjugated segment, a larger number of conjugated coplanar repeating units makes a structural local site for excitons with a lower electronic energy. In our **P3HT** TA measurements, the excitation wavelength of 510 nm is at the red edge of the $S_1 \leftarrow S_0$ transition band, which selectively creates the lowest energy excitons located in the longest conjugated segments in the polymer backbone. Because of the identical thiophene blocks and hence strong electronic couplings between adjacent repeating units when the polymer backbone is planar, the initial excitons can delocalize to neighboring sites with similar energetics. Conversely, the lack of the fast component in the TAA result of **P3HT** shows that the fast exciton diffusion of the initial excitons is prohibited, which seems to contradict the statement regarding strong electronic coupling between identical and adjacent thiophene units. This inconsistency can be explained by our red-edge excitation using the 510 nm light, which preferentially generates the initial excitons with the longest conjugation and the lowest electronic energies. As observed in previous work by others, the planarity will be enhanced in the excitonic state compared to the ground state due to the formation of the quinoidal character that enhances the bond order between the repeating units in **P3HT**. Due to the C−C bond rotations in other parts of the **P3HT** backbone that disrupt the π-conjugation, these low energy excitons on the long segments are structurally and energetically isolated by neighboring shorter conjugated segments with higher electronic energies, hence their diffusion along the polymer backbone will be energetically uphill and prohibited. In this work, we confirm that there is no depolarization process caused by exciton diffusion or structural deformation in **P3HT** within a few picoseconds. Meanwhile, the result also suggests that the selection of excitation wavelength for an optical experiment of heterogeneous OPV polymers is very important because it is directly related to energetic and structural factors of the initial excitons. Therefore, our results are not contradictory to the previous works and the experimental inconsistency is mainly due to the shorter excitation wavelength and subsequent complex energetic and structural heterogeneities.[14,33,35]

The slow depolarization component of 34 ps is likely due to a long-range incoherent exciton diffusion to an energetic global minimum following conformational changes of the polymer backbone in solution, as shown in previous works.[33,36] It is hard to assign the relative portion between the incoherent exciton diffusion and the conformational motion. Although there is no fast exciton diffusion, the small r_∞ value of **P3HT** is related to structural factors such as structural inhomogeneity and flexibility between constituent units. Moreover, the origins of two fast energetic relaxation processes shown in the isotropic TA trace of **P3HT** could be originated from vibrational relaxation and solvent mediated deactivation dynamics, respectively, which are not related to the reorientation of transition dipole moment.

Exciton Dynamics in PTB7. The fastest components of <100 fs are present in both the isotropic TA and TAA signals of **PTB7** exciton dynamics, which report the first initial exciton decay process detectable in our experiments. Interestingly, the TAA decay dynamics of **PTB7** are excitation energy dependent. The amplitude of the fastest TAA decay component increases with the excitation energy. After photoexcitation at 600 nm, the TAA amplitude of the fastest depolarization component becomes larger compared to that at 700 nm excitation and a new depolarization component of 320 fs appears. Since the excitation at 600 nm induces the transition to the S_1 state that is approximately one vibrational quanta higher in energy than that by the direct excitation to the 0−0 transition at 700 nm, the possible dynamic processes from an excited vibronic state are vibrational relaxation and exciton diffusion, as well as the formation of the PCT and CS states. Because the fastest TAA decay time constant under the 600 or 700 nm excitation is <50 fs, much shorter than vibrational relaxation in solution, the

DOI: 10.1021/jp5111345
J. Phys. Chem. B XXXX, XXX, XXX−XXX

larger TAA amplitude indicates that initial excitons are more efficiently diffused or the CS or PCT forms more favorably. In order to find an answer to the question about the origin of the fastest depolarization process before vibrational relaxation, we also consider other possible physical phenomena. It has been proposed dynamic exciton localization on this time scale along twisted segments in fully conjugated PPV (polyphenyleneviny-lene) polymers in chlorobenzene.[37] Since the backbone of **PTB7** is relatively rigid according to its large $r(t)$ value at long delay time, that is, 80 ps, the local environments for each repeating unit are relatively homogeneous as rationalized from the clear vibronic features in the absorption bands. Thus, the dynamic exciton localization along twisted segments does not agree with our experimental observations. The other possibilities would be ultrafast thermalization of the mobile electrons and holes toward the band edges and their self-localization,[38,39] and coherent intrachain exciton migration through the π-stacks[31] in the direction perpendicular to the transition dipole moment direction. As previously mentioned, we are convinced that the initial state is an emissive exciton state and that CS state cannot contribute to SE in our TA signals. Our experimental and theoretical results suggest that **PTB7** is structurally more homogeneous and more rigidly stretched in solution than **P3HT**. On one hand, these characteristic **PTB7** structural factors can lead to delocalization of excitons in favor of efficient exciton diffusion to the neighboring exciton sites. On the other hand, the electron density is more localized in oligomer corresponding to **PTB7** that that to **P3HT** as shown in our calculations due to the electronic and symmetric differences between the two adjacent blocks, such as **BDT** and **TT**, which retard the exciton diffusion. In addition, the initial excitons with excess energy higher than the activation barriers between neighboring exciton sites will be able to diffuse through the polymer chain efficiently. Therefore, a larger portion of the initial excitons in **PTB7** after photoexcitation at 600 nm can coherently diffuse than those under the red-edge excitation at 700 nm. Once the excess energy surpasses the activations barriers for the exciton hopping, the barriers have no effect on coherent exciton diffusion. The larger TAA amplitude of the fastest depolariza-tion component at 600 nm supports this mechanism, that a high excitation energy and subsequent high excess energy of initial excitons are important to accelerate the coherent depolarization process. As mentioned earlier, we cannot rule out the exciton hopping through the π-stacks and such processes can be coherent if the wave functions between the stacked chains overlap and take place in tens of fs as shown in Rossky's calculations for PPV.[31] Consequently, we suggest that most of the initial excitons coherently diffuse through neighboring local sites before vibrational relaxation and that this coherent diffusion process becomes more efficient by the higher excess energy of initial excitons. The other initial excitons undergo intrachain/interchain charge transfer/charge separation to form PCT and CS states within less than 100 fs, as we previously observed as well as coherent diffusion through interchain π-stacks. This process was also found to be excitation wavelength independent in solution, while the relative ratio of CS/PCT is dependent on local structure as described in our previous studies.[17] Considering that the previous work was carried out with an IRF of 160 fs, it is not surprising that the excitation wavelength dependence that only appears in the fastest components were missed in our earlier work.

After vibrational relaxation, the thermalized exciton diffusion starts from the zeroth vibrational state and can be understood as an incoherent process because there is an activation energy barrier for exciton diffusion. We initially hypothesized that fast structural variations, such as conformational and rotational motions, could contribute to depolarization processes. How-ever, the TAA signals of **P3HT** shows no sign of fast depolarization components within a few picoseconds and, hence, hardly depend on structural motions on that time scale. In contrast, the second and third remaining depolarization components of 320 fs and 2.6 ps in **PTB7**, which are similar to previous result of an alternating polymer,[38] are presumably caused by incoherent exciton hopping processes, which also correspond to single step exciton hopping time.[34] Since the second depolarization component is only shown at the excitation wavelength at 600 nm and not shown in the isotropic TA trace, its origin is not clear but it is certain that this process is also an incoherent diffusion process after vibrational relaxation. If we assume a structural intrinsic inhomogeneity of **PTB7**, it is possible that the fast and slow incoherent hopping processes are caused by different local positions of excitons with various conjugation lengths. On the other hand, the fourth depolarization component in **PTB7** can be understood as incoherent exciton diffusion and conformational motion of a polymer backbone like **P3HT**. Although the molecular local structure of **PTB7** is expected to be rigid, the fourth depolarization time is faster than that of relatively flexible **P3HT**, reflecting that the incoherent exciton diffusion contributes mainly to the fourth depolarization component.

Scheme 2 shows a simplified diagram for the overall exciton diffusion processes in **PTB7**. There are many exciton local sites

Scheme 2. Schematic Diagram of Coherent and Incoherent Exciton Diffusion Processes in PTB7[a]

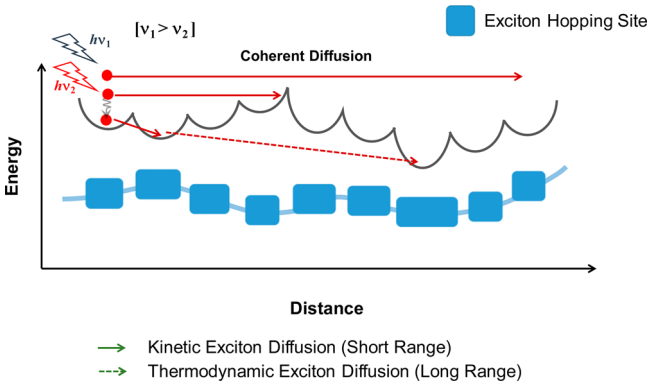

[a]The lengths of exciton hopping sites (blue boxes) present the numbers of coupled **TT** and **BDT** units.

with various energy levels depending on the local structures and the number of coupled constituent units. Considering two possible exciton dynamic processes from the initial excitons with high and low excess energies after photoexcitation, while the former can diffuse over activation barriers before the vibrational relaxation, the latter with low energy or thermally relaxed excitons have to climb or tunnel through an activation barrier to diffuse. If the initial excitons have high excess energies, they can coherently diffuse or delocalize in relatively long fragments. After vibrational relaxation, there are short-range exciton diffusions to neighboring local sites with similar energy or with an energetic local minimum (kinetic process)

DOI: 10.1021/jp5111345
J. Phys. Chem. B XXXX, XXX, XXX−XXX

and finally long-range exciton diffusion to a local site with a global minimum (thermodynamic process). These incoherent exciton diffusions take place sequentially depending on their time scales and the homogeneous local hopping sites with similar energies in **PTB7** seem to be an important factor for efficient incoherent diffusion.

V. CONCLUSION

We have investigated the energy relaxation and exciton diffusion dynamics of **P3HT** and **PTB7** polymers that are commonly used in the active layers of organic photovoltaic devices. According to the dynamics in both TA and TAA measurements, we found that the excitons in these polymers can diffuse coherently and incoherently depending on their excess energy gained from the photoexcitation. **P3HT** excitons with little excess energy exhibit only the single-exponential depolarization component of 34 ps in the TAA signal, indicating that there is no fast conformational change within a few picoseconds and that the initial excitons at long conjugated local sites with low electronic energies cannot diffuse. In comparison, **PTB7** shows multiple and sequential exciton diffusion dynamics, which are affected by the excitation excess energies of the initial excited state. The excess energy of the initial excited state induces the acceleration of coherent exciton diffusion and the extra electronic relaxations to PCT and CS states. The self-aggregation induced backbone rigidity and planarization of **PTB7** cause the reduction of structurally and energetically inhomogeneity in solution and films, which then can enforce various coherent and incoherent exciton diffusion pathways. Such structural characters are probably related to the extended exciton diffusion length through the polymer backbone as well as π-stacking, which are absent in **P3HT**. This work will serve as a firm basis for future studies on energy relaxation and exciton diffusion dynamics of OPV polymers.

■ ASSOCIATED CONTENT

Supporting Information

Instrument response curve and calculated molecular orbitals for the oligomers. This material is available free of charge via the Internet at http://pubs.acs.org.

■ AUTHOR INFORMATION

Corresponding Authors

*E-mail: lchen@anl.gov.

*E-mail: lupingyu@uchicago.edu.

Notes

The authors declare no competing financial interest.

■ ACKNOWLEDGMENTS

This research is supported by the ANSER Center, an Energy Frontier Research Center funded by the U.S. Department of Energy, Office of Science, Office of Basic Energy Sciences, under Award Number DE-SC0001059. The laser system for the study is supported by the Division of Chemical Sciences, Office of Basic Energy Sciences, the U.S. Department of Energy under Contract DE-AC02-06CH11357 (for L.X.C.). S.C. acknowledges Basic Science Research Program through the National Research Foundation of Korea (NRF) funded by the Ministry of Education (2013R1A1A2062226). We thank Mr. Nicholas Jackson for reading the manuscript and providing useful comments.

■ REFERENCES

(1) Friend, R. H.; Gymer, R. W.; Holmes, A. B.; Burroughes, J. H.; Marks, R. N.; Taliani, C.; Bradley, D. D. C.; Santos, D. A. D.; Brédas, J. L.; Lögdlund, M.; Salaneck, W. R. Electroluminescence in Conjugated Polymers. *Nature* **1999**, *397*, 121.

(2) Forrest, S. R. The Path to Ubiquitous and Low-Cost Organic Electronic Appliances on Plastic. *Nature* **2004**, *428*, 911.

(3) Murphy, A. R.; Fréchet, J. M. J. Organic Semiconducting Oligomers for Use in Thin Film Transistors. *Chem. Rev.* **2007**, *107*, 1066−1096.

(4) Günes, S.; Neugebauer, H.; Sariciftci, N. S. Conjugated Polymer-Based Organic Solar Cells. *Chem. Rev.* **2007**, *107*, 1324.

(5) Heeger, A. J. Semiconducting Polymers: The Third Generation. *Chem. Soc. Rev.* **2010**, *39*, 2354−2371.

(6) Dennler, G.; Scharber, M. C.; Brabec, C. J. Polymer-Fullerene Bulk-Heterojunction Solar Cells. *Adv. Mater.* **2009**, *21*, 1323.

(7) Halls, J. J. M.; Walsh, C. A.; Greenham, N. C.; Marseglia, E. A.; Friend, R. H.; Moratti, S. C.; Holmes, A. B. Efficient Photodiodes from Interpenetrating Polymer Networks. *Nature* **1995**, *376*, 498.

(8) Yu, G.; Gao, J.; Hummelen, J. C.; Wudl, F.; Heeger, A. J. Polymer Photovoltaic Cells: Enhanced Efficiencies via a Newwork of Internal Donor-Acceptor Heterojunctions. *Science* **1995**, *270*, 1789−1791.

(9) Scharber, M. C.; Sariciftci, N. S. Efficiency of Bulk-Heterojunction Organic Solar Cells. *Prog. Polym. Sci.* **2013**, *38*, 1929−1940.

(10) Forrest, S. R. The Limits to Organic Photovoltaic Cell Efficiency. *MRS Bull.* **2005**, *30*, 28−31.

(11) Brédas, J.-L.; Norton, J. E.; Cornil, J.; Coropceanu, V. Molecular Understanding of Organic Solar Cells: The Challenges. *Acc. Chem. Res.* **2009**, *42*, 1691.

(12) Heremans, P.; Cheyns, D.; Rand, B. P. Strategies for Increasing the Efficiency of Heterojunction Organic Solar Cells: Material Selection and Device Architecture. *Acc. Chem. Res.* **2009**, *42*, 1740−1747.

(13) Banerji, N.; Seifter, J.; Wang, M.; Vauthey, E.; Wudl, F.; Heeger, A. J. Ultrafast Spectroscopic Investigation of a Fullerene Poly(3-hexylthiophene) Dyad. *Phys. Rev. B* **2011**, *84*, 075206.

(14) Banerji, N.; Cowan, S.; Vauthey, E.; Heeger, A. J. Ultrafast Relaxation of the Poly(3-hexylthiophene) Emission Spectrum. *J. Phys. Chem. C* **2011**, *115*, 9726.

(15) Guo, J.; Ohkita, H.; Benten, J.; Ito, S. Charge Generation and Recombination Dynamics in Poly(3-hexylthiopehen)/Fullerene Blend Films with Different Regioregularities and Morphologies. *J. Am. Chem. Soc.* **2010**, *132*, 6154−6164.

(16) Kaake, L. G.; Jasieniak, J. J.; R. C. Bakus, I.; Welch, G. C.; Moses, D.; Bazan, G. C.; Heeger, A. J. Photoinduced Charge Generation in a Molecular Bulk Heterojunction Material. *J. Am. Chem. Soc.* **2012**, *134*, 19828−19838.

(17) Rolczynski, B. S.; Szarko, J. M.; Son, H. J.; Liang, Y.; Yu, L.; Chen, L. X. Ultrafast Intramolecular Exciton Splitting Dynamics in Isolated Low-Band-Gap Polymers and Their Implications in Photovoltaic Materials Design. *J. Am. Chem. Soc.* **2012**, *134*, 4142−4152.

(18) Rolczynski, B. S.; Szarko, J. M.; Son, H. J.; Yu, L. P.; Chen, L. X. Effects of Exciton Polarity in Charge-Transfer Polymer/PCBM Bulk Heterojunction Films. *J. Phys. Chem. Lett.* **2014**, *5*, 1856−1863.

(19) Liang, Y.; Xu, Z.; Xia, J.; Tsai, S.-T.; Wu, Y.; Li, G.; Ray, C.; Yu, L. For the Bright Future-Bulk Heterojunction Polymer Solar Cells with Power Conversion Efficiency of 7.4%. *Adv. Mater.* **2010**, *22*, E135−E138.

(20) Cho, S.; Mara, M. W.; Wang, X.; Lockard, J. V.; Rachford, A. A.; Castellano, F. N.; Chen, L. X. Coherence in Metal-Metal-to-Ligand-Charge-Transfer Excited States of a Dimetallic Complex Investigated by Ultrafast Transient Absorption Anisotropy. *J. Phys. Chem. A* **2011**, *115*, 3990.

(21) Cook, S.; Furube, A.; Katoh, R. Analysis of the Excited States of Regioregular Polythiophene P3HT. *Energy Environ. Sci.* **2008**, *1*, 294.

(22) Louarn, G.; Trznadel, M.; Buisson, J. P.; Laska, J.; Pron, A.; Lapkowski, M.; Lefrant, S. Raman Spectroscopic Studies of

DOI: 10.1021/jp5111345
J. Phys. Chem. B XXXX, XXX, XXX−XXX

Regioregular Poly(3-alkylthiophenes). *J. Phys. Chem.* **1996**, *100*, 12532−12539.
(23) Heffner, G. W.; Pearson, D. S. Molecular Characterization of Poly(3-hexylthiphene). *Macromolecules* **1991**, *24*, 6295−6299.
(24) Tahiro, K.; Ono, K.; Minagawa, Y.; Kobayashi, M.; Kawai, T.; Yoshino, K. Structure and Thermochromic Solid-State Phase Transition of Poly(3-alkylthiophene). *J. Polym. Sci.* **1991**, *29*, 1223−1233.
(25) DuBay, K. H.; Hall, M. L.; Hughes, T. F.; Wu, C.; Reichman, D. R.; Friesner, R. A. Accurate Force Field Development for Modeling Conjugated Polymers. *J. Chem. Theory Comput.* **2012**, *8*, 4556−4569.
(26) Jackson, N. E.; Savoie, B. M.; Kohlstedt, K. L.; de la Cruz, M. O.; Schatz, G. C.; Chen, L. X.; Ratner, M. A. Controlling Conformations of Conjugated Polymers and Small Molecules: The Role of Nonbonding Interactions. *J. Am. Chem. Soc.* **2013**, *135*, 10475−10483.
(27) Szarko, J. M.; Rolczynski, B. S.; Lou, S. J.; Xu, T.; Strzalka, J.; Marks, T. J.; Yu, L. P.; Chen, L. X. Photovoltaic Function and Exciton/Charge Transfer Dynamics in a Highly Efficient Semiconducting Copolymer. *Adv. Funct. Mater.* **2014**, *24*, 10−26.
(28) Rolczynski, B. S.; Szarko, J. M.; Son, H. J.; Liang, Y.; Yu, L.; Chen, L. X. Effects of Intramolecular Exciton Dynamics in Charge-Transfer Polymer Organic Photovoltaic Devices. *J. Phys. Chem. Lett.* **2014**, *5*, 1856−1863.
(29) Huo, M.-M.; Liang, R.; Xing, Y.-D.; Hu, R.; Zhao, N.-J.; Zhang, W.; Fu, L.-M.; Ai, X.-C.; Zhang, J.-P.; Hou, J.-H. Side-Chain Effects on the Solution-Phase Conformations and Charge Photogeneration Dynamics of Low-Bandgap Copolymers. *J. Chem. Phys.* **2013**, *139*, 124904 (124914).
(30) Hu, Z. J.; Adachi, T.; Haws, R.; Shuang, B.; Ono, R. J.; Bielawski, C. W.; Landes, C. F.; Rossky, P. J.; Vanden Bout, D. A. Excitonic Energy Migration in Conjugated Polymers: The Critical Role of Interchain Morphology. *J. Am. Chem. Soc.* **2014**, *136*, 16023−16031.
(31) Bedard-Hearn, M. J.; Sterpone, F.; Rossky, P. J. Nonadiabatic Simulations of Exciton Dissociation in Poly-p-phenylenevinylene Oligomers. *J. Phys. Chem. A* **2010**, *114*, 7661−7670.
(32) Lou, S. J.; Szarko, J. M.; Xu, T.; Yu, L.; Marks, T. J.; Chen, L. X. Effects of Additives on the Morphology of Solution Phase Aggregates Formed by Active Layer Components of High-Efficiency Organic Solar Cells. *J. Am. Chem. Soc.* **2011**, *133*, 20661−20663.
(33) Xie, Y.; Li, Y.; Xiao, L.; Qiao, Q.; Dhakal, R.; Zhang, Z.; Gong, Q.; Galipeau, D.; Yan, X. Femtosecond Time-Resolved Fluorescence Study of P3HT/PCBM Blend Films. *J. Phys. Chem. C* **2010**, *114*, 14590−14600.
(34) Nakamura, T.; Araki, Y.; Ito, O.; Takimiya, K.; Otsubo, T. Fluorescence Up-Conversion Study of Excitation Energy Transport Dynamics in Oligothiophene-Fullerene Linked Dyads. *J. Phys. Chem. A* **2008**, *112*, 1125−1132.
(35) Wells, N. P.; Blank, D. A. Correlated Exciton Relaxation in Poly(3-hexylthiophene). *Phys. Rev. Lett.* **2008**, *100*, 086403(086404).
(36) Westenhoff, S.; Daniel, C.; Friend, R. H.; Silva, C.; Sundström, V.; Yartsev, A. Exciton migration in a polythiophene: Probing the Spatial and Energy Domain by Line-Dipole Förster-Type Energy Transfer. *J. Chem. Phys.* **2005**, *122*, 094903.
(37) Ruseckas, A.; Wood, P.; Samuel, I. D. W.; Webster, G. R.; Mitchell, W. J.; Burn, P. L.; Sundström, V. Ultrafast Depolarization of the Fluorescence in a Conjugated Polymer. *Phys. Rev. B* **2005**, *72*, 115214.
(38) Banerji, N.; Cowan, S.; Leclerc, M.; Vauthey, E.; Heeger, A. J. Exciton Formation, Relaxation, and Decay in PCDTBT. *J. Am. Chem. Soc.* **2010**, *132*, 17459.
(39) Collini, E.; Scholes, G. D. Coherent Intrachain Energy Migration in a Conjugated Polymer at Room Temperature. *Science* **2009**, *323*, 369.

DOI: 10.1021/jp5111345
J. Phys. Chem. B XXXX, XXX, XXX−XXX